JOURNAL OF SOLID STATE CHEMISTRY 60, 237–243 (1985)

Gibbs Energy of Formation of Cobalt Divanadium Tetroxide

K. T. JACOB AND S. SHASHIDHARA PANDIT

Department of Metallurgy, Indian Institute of Science, Bangalore 560 012, India

Received April 29, 1985

The Gibbs energy of formation of V_2O_3-saturated spinel CoV_2O_4 has been measured in the temperature range 900–1700 K using a solid state galvanic cell, which can be represented as Pt, Co + CoV_2O_4 + V_2O_3/(CaO) ZrO_2/Co + CoO, Pt. The standard free energy of formation of cobalt vanadite from component oxides can be represented as CoO (rs) + V_2O_3 (cor) → CoV_2O_4 (sp), $\Delta G^\circ = -30{,}125 - 5.06T$ (± 150) J mole^{-1}. Cation mixing on crystallographically nonequivalent sites of the spinel is responsible for the decrease in free energy with increasing temperature. A correlation between "second law" entropies of formation of cubic 2–3 spinels from component oxides with rock salt and corundum structures and cation distribution is presented. Based on the information obtained in this study and trends in the stability of aluminate and chromite spinels, it can be deduced that copper vanadite is unstable.

Introduction

As part of a larger program of research on thermodynamic properties of spinels and their relation to electronic and crystallographic structure, the stability of cobalt vanadium tetroxide (cobalt vanadite) has been measured using a galvanic cell incorporating calcia-stabilized zirconia solid electrolyte. The Gibbs energy of formation of this compound was determined by Kunnmann *et al.* (*1*) from 1073 to 1380 K using CO/CO_2 gas mixtures. Recent solid-state electrochemical studies (*2*) have revealed significant systematic errors in the measurements of Kunnmann *et al.* on iron chromite ($FeCr_2O_4$) and iron vanadite (FeV_2O_4) using the same technique. Since solid-state cells provide greater accuracy in thermodynamic studies on oxides compared to the older CO/CO_2 equilibrium technique, the former method was selected in this study.

Cobalt vanadite forms as a deoxidation product in the liquid Co–V–O system. A knowledge of its Gibbs energy of formation is useful for delineating the conditions of its formation. The deoxidizing power of vanadium is enhanced by the formation of the spinel rather than vanadium sesquioxide.

Experimental Methods

Materials

Fine powders of cobalt (99.99%), cobalt monoxide (99.99%), and vanadium sesquioxide (99.9%) were obtained from Alfa Inorganics. Cobalt vanadite was prepared by prolonged heating of pressed pellets containing CoO and V_2O_3 in equimolar ratio for 3 to 4 days at 1400 K. The pellets were contained in alumina crucibles placed inside evacuated silica capsules. The pellets were crushed after cooling, recompacted

0022-4596/85 $3.00

and heated again under vacuum. Formation of cobalt vanadite was confirmed by X-ray diffraction analysis. Impervious calcia-stabilized zirconia tubes used in this study contained 15 mole% CaO. The high purity argon gas was dried and deoxidized by passing it through a column of titanium granules maintained at 1100 K before being used to provide an inert atmosphere around the emf cell.

Apparatus and Procedure

The reversible emf of the following cells were measured as a function of temperature in the range 900 to 1700 K,

$$\text{Pt, Co + CoO/(CaO)ZrO}_2\text{/O}_2\text{, Pt} \quad \text{(I)}$$

$$\text{Pt, Co + CoV}_2\text{O}_4\text{ + V}_2\text{O}_3\text{/(CaO)ZrO}_2\text{/Co + CoO, Pt} \quad \text{(II)}$$

where the right-hand electrode is positive.

The condensed phase electrodes were prepared by mixing fine powders of component metals and oxides in equimolar proportions, compacting the mixture into pellets and sintering in evacuated quartz capsules at 1400 K. Examination of the pellets by optical microscopy and X-ray diffraction showed that the initial phases were preserved during sintering. The pellets were polished and spring loaded against flat-end calcia-stabilized zirconia tube. The oxygen electrode in cell I was prepared by painting the outer surface of calcia-stabilized zirconia tube with platinum powder (−325 mesh), suspended in an organic liquid followed by drying at room temperature and sintering in air for 8 hr at 1300 K. Platinum–lead wires were attached to the porous platinum electrode by sintering. The apparatus and cell arrangement were similar to that used earlier (*3*).

The oxygen reference gas in cell I was maintained at a pressure of 101325 Pa by adjusting the mercury level at the exit. The importance of correcting for atmospheric pressure variations in accurate measurements using a gaseous reference electrode has been overlooked in a number of investigations. The emf of the cells were measured with a Princeton Applied Research (Model PAR 136) high-impedance digital voltmeter. The condensed phases were maintained under flowing argon gas. The reversibility of the cells were checked by passing small currents (~50 μA) through the cell in either direction for upto 200 sec. In each case the emf was found to return to the original value before coulometric titration. The emf was also independent of the flow rate of oxygen and/or argon gas through the cell in the range 1 to 3 ml sec^{-1}.

The temperature of the cell was measured by a Pt/Pt–13% Rh thermocouple placed adjacent to the electrodes. To check for the absence of thermal gradients, the emf of a symmetric cell with two identical Co + CoO electrodes was measured as a function of temperature from 900 to 1700 K. The emf was less than ±0.2 mV at all temperatures without any systematic trends. The electrodes were examined at the end of each experiment by X-ray diffraction to identify any new phases that might have formed during emf measurement. In all cases the phase composition of the electrodes were unchanged.

After a change in temperature, the emf of cell I attained equilibrium values in 1 to 3 hr depending on temperature. Corresponding times for cell II ranged from 12 hr at 900 K to 2 hr at 1700 K. The slow response of cell II was due to kinetics of reaction between three condensed phases at the left-hand electrode. Application of an ac voltage with an amplitude of 50 mV was found to shorten the time required to attain steady emf by a factor of 3 in the temperature range 900 to 1300 K. In each case, the cell emf was monitored for 2 to 6 hr after the removal of ac potential. Application of ac at temperatures above 1300 K was found to accelerate the limited reaction between cobalt oxide and the solid electrolyte. The ex-

act mechanisms by which the ac potential facilitates faster equilibration at the electrodes have not been established. A tentative explanation may be offered as follows. At the interface between the three-phase electrode and the solid electrolyte, there may initially be an inhomogeneity in oxygen potential. When an ac voltage is applied, oxygen is removed during a half cycle mainly from high oxygen potential regions of the interface. During the next half cycle oxygen is pumped back to this interface, presumably to the low oxygen potential regions. Although the amounts transported in each half cycle may differ because of the differing polarization characteristics of the electrodes, the net effect is to homogenize the oxygen potential at the electrode/electrolyte interface.

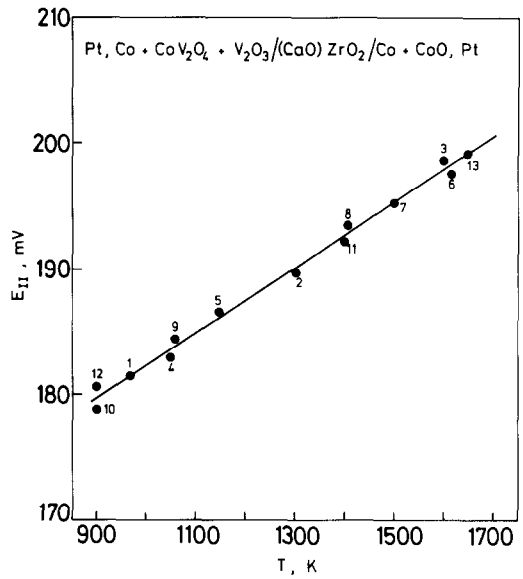

FIG. 2. Variation of the emf of cell II with temperature.

Results

The reversible emfs of cells I and II are plotted as a function of temperature in Figs. 1 and 2, respectively. The sequence of measurements is indicated by numbers on the graphs. The emf of cell I shows a scatter of ±0.5 mV, while the potential of cell II exhibits a reproducibility of ±0.8 mV. The least-squares regression analysis gives the following equations for emf of cells I and II:

$$E_{\mathrm{I}} = 1{,}215.7 - 0.368T \text{ mV} \quad (1)$$

$$E_{\mathrm{II}} = 156.1 + 0.0262T \text{ mV}. \quad (2)$$

The Gibbs energy of formation of CoO and V_2O_3-saturated CoV_2O_4 from component oxides can be evaluated from the emf data:

$$\mathrm{Co\ (fcc)} + \tfrac{1}{2}\mathrm{O_2\ (g)} \rightarrow \mathrm{CoO\ (rs)}$$

$$\Delta G^\circ = -234{,}620 + 71.02T\ (\pm 100)\ \mathrm{J\ mole^{-1}} \quad (3)$$

$$\mathrm{CoO\ (rs)} + \mathrm{V_2O_3\ (cor)} \rightarrow \mathrm{CoV_2O_4\ (sp)}$$

$$\Delta G^\circ = -30{,}125 - 5.06T\ (\pm 150)\ \mathrm{J\ mole^{-1}}. \quad (4)$$

The error limits correspond to twice the standard deviation. The absolute accuracy is more difficult to evaluate. Considering possible errors in temperature and emf

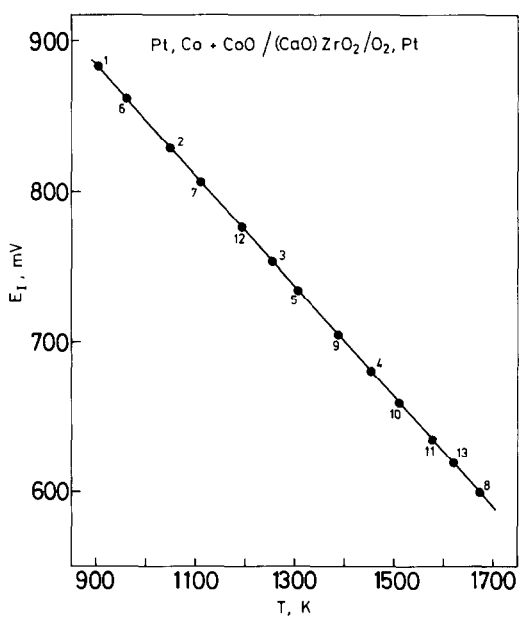

FIG. 1. Temperature dependence of the emf of cell I.

measurements, it is estimated that absolute error limits are higher by a factor of 2. By combining Eqs. (3) and (4), the oxygen potential corresponding to the left-hand, three-phase electrode in cell II can be obtained:

$$\text{Co (fcc)} + \tfrac{1}{2}O_2\text{ (g)} + V_2O_3\text{ (cor)} \rightarrow CoV_2O_4\text{ (sp)}$$

$$\Delta G^\circ = -264{,}745 + 65.96T\ (\pm 180)\ \text{J mole}^{-1}. \quad (5)$$

Discussion

(a) Gibbs Energy of Formation of Cobalt Oxide

The standard Gibbs energy of formation of cobalt monoxide is well established (*4–8*). The main purpose of measurements on cell I was to calibrate the emf apparatus. Gibbs energy of formation of cobalt oxide obtained in this study is compared in Table I with some classic results reported in the literature (*4–7*) and recent JANAF (*8*) values. The results of this study agree with the evaluated data of Janaf within 400 J mole^{-1}, suggesting that the absolute accuracy in measurement is of this order.

(b) Gibbs Energy of Formation of Cobalt Vanadite

The oxygen potential corresponding to the equilibrium between Co, CoV_2O_4, and V_2O_3 given in Eq. (5) is plotted as a function of temperature in Fig. 3 along with the results of Kunnmann *et al.* (*1*) obtained by a CO/CO_2 equilibration technique. The data of Kunnmann *et al.* are 24 to 17 kJ more positive. Similar discrepancies have been found between recent emf measurements (*2*) and the earlier gas equilibrium study for other spinel phases such as FeV_2O_4 and $FeCr_2O_4$. The emf data for a number of spinel compounds are compatible with available calorimetric information (*11–14*). The oxygen potentials corresponding to formation of higher oxides in the V–O system are also shown in Fig. 3. Clearly V_2O_3 is the stable binary oxide in equilibrium at the oxygen potentials established by the decomposition of CoV_2O_4.

The increase in the stability of CoV_2O_4, with respect to component oxides CoO and V_2O_3 with increasing temperature, apparent in Fig. 2 and Eq. (4), is an interesting feature. The solid-state reactions between two binary oxides to form the ternary com-

TABLE I

COMPARISON OF GIBBS ENERGY OF FORMATION OF CoO FROM DIFFERENT SOURCES; $Co + \frac{1}{2}O_2 \rightarrow CoO$; ΔG°, kJ

Reference	Temperature (K)			
	900	1100	1300	1500
Kiukkola & Wagner (*4*) emf (1957)	—	−157.02	−142.76	—
Aukrust & Muan (*5*) Gas equi. (1963)	—	—	−144.75	−130.11
Tretjakow & Schmalzried (*6*) emf (1965)	−165.33	−155.24	−139.73	−124.22
Myers and Gunter (*7*) emf (1979)	−171.55	−156.392	−141.140	−126.090
Chase *et al.* (*8*) Janaf (1974)	−170.280	−156.398	−142.495	−128.407
This study emf	−170.702	−156.498	−142.294	−128.09

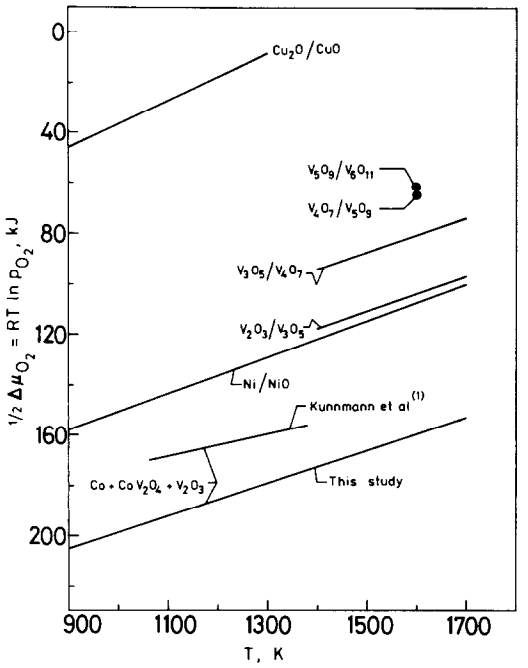

FIG. 3. Comparison of the measured oxygen potential for condensed phase equilibrium between Co, CoV_2O_4, and V_2O_3 and the values of Kunnmann *et al.* (*1*), as a function of temperature. The oxygen potentials corresponding to two phase equilibria in the binary V–O, Cu–O, and Ni–O systems are also shown.

pound (CoV_2O_4) is accompanied by a significant positive entropy change. The higher entropy of the spinel phase may arise from cation mixing in tetrahedral and octahedral sites in the structure.

Although V_2O_3 is a nonstoichiometric oxide with a wide homogeneity ranging up to an O/V ratio of 1.56 at 1700 K (*9, 10*), at the oxygen potentials measured in this study it is essentially stoichiometric. The spinel phase, however, may dissolve some excess V_2O_3, and its composition may be more accurately written as $CoV_{2+2x}O_{4+3x}$. The measurements correspond to the V_2O_3-saturated spinel. The value of x is not available in the literature. Attempts to measure x using a microprobe did not give reproducible results.

(c) *Cation Distribution and Entropy of Formation*

In the absence of direct cation distribution measurements on CoV_2O_4 at high temperatures, the fraction of divalent cobalt ion on the tetrahedral site (λ) may be estimated from octahedral site preference energies (H^{oct}) of Co^{2+} and V^{3+} ions given by crystal field theory (*15*). It has been shown earlier (*2, 15*) that

$$H^{oct}_{Co^{2+}} - H^{oct}_{V^{3+}} = \Delta H^{ex} = -RT \ln \frac{(1-\lambda)^2}{\lambda(1+\lambda)} \quad (6)$$

where $\Delta H^{ex} = 22.6$ kJ (*15*) is the enthalpy change for the exchange reaction,

$$(Co^{2+})_{tet} + [V^{3+}]_{oct} \rightarrow [Co^{2+}]_{oct} + (V^{3+})_{tet} \quad (7)$$

and cation disorder is represented as $(Co_\lambda V_{1-\lambda})_{tet}[Co_{1-\lambda}V_{1+\lambda}]_{oct}O_4$. The value of λ at a mean experimental temperature of 1300 K calculated using the above equation is 0.64, close to the random composition (λ = 0.667), corresponding to maximum entropy. Assuming ideal Temkin mixing on both cationic sublattices, the configurational entropy of the crystal is given by

$$\Delta S^{CM} = -R\left[\lambda \ln\lambda + (1-\lambda)\ln(1-\lambda) + (1-\lambda)\ln\frac{(1-\lambda)}{2} + (1+\lambda)\ln\frac{(1+\lambda)}{2}\right]$$

$$= 13.22 \text{ J K}^{-1} \text{ mole}^{-1}. \quad (8)$$

It had been suggested earlier (*14*) that the entropy of formation of cubic 2–3 spinels from component oxides with rock salt and corundum structures can be represented by

$$\Delta S^\circ_f = -7.32 + \Delta S^{CM} + \Delta S^{rand}_{J-T} \text{ J K}^{-1} \text{ mole}^{-1} \quad (9)$$

where ΔS^{CM} is the configurational entropy of the crystal due to cation mixing and $\Delta S^{rand}_{J-T} = nR \ln 3$, is the entropy associated

with randomizing the direction of Jahn–Teller distortions. The number of moles of the distorting ion on a site is represented by n. The Jahn–Teller term appears to apply only to spinel phases that have $3d^4$ or $3d^9$ configuration in the octahedral site or $3d^3$, $3d^4$, $3d^8$, or $3d^9$ ions in the tetrahedral coordination. The presence of distorting ions is generally manifested by a transition from cubic to tetragonal symmetry at low temperatures. In a few crystals like $CuAl_2O_4$, the opposing effect of the Cu^{2+} ion on octahedral and tetrahedral sites allows the cubic symmetry to prevail at room temperature.

The entropy of formation of CoV_2O_4 from component oxides obtained from measurement is 5.06 J K^{-1} $mole^{-1}$ in good agreement with 5.9 J K^{-1} $mole^{-1}$ given by the empirical correlation (Eq. (9)). Information on second-law entropies of formation of cubic 2–3 spinels from component oxides with rock salt and corundum structures is plotted in Fig. 4 as a function of $-7.32 + \Delta S^{CM}$ (first two terms on right hand side of Eq. (9)). Data for all the compounds except Fe_3O_4 are from emf measurements—published (*2, 11–14*) and unpublished (*15*). Information on Fe_3O_4 is from JANAF tables (*17*). Of all the compounds considered, only $NiCr_2O_4$ has a substantial Jahn–Teller contribution (~8.7 J K^{-1} $mole^{-1}$). For $NiAl_2O_4$ the Jahn–Teller contribution is only 1.8 J K^{-1} $mole^{-1}$. The results shown in Fig. 4 clearly establish quantitatively the effect of cation mixing on entropy of formation.

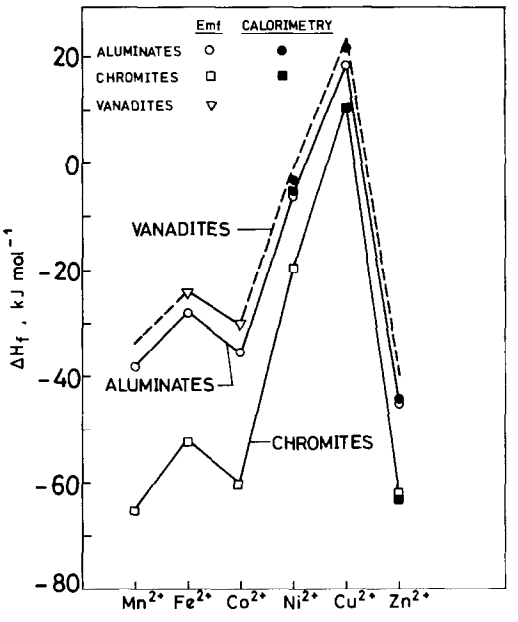

FIG. 5. Empirical trends in the enthalpy of formation of cubic 2–3 spinels from component oxides.

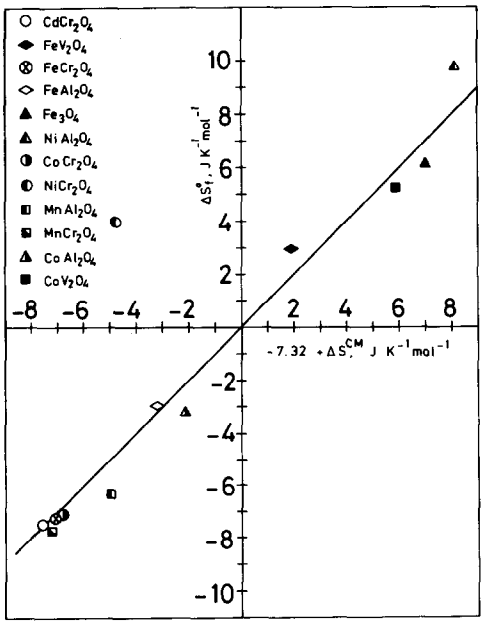

FIG. 4. Correlation between measured entropy of formation of cubic 2–3 spinels from component oxides with rock salt and corundum structures (ΔS_f°) and cation mixing entropy of spinels (ΔS^{CM}).

(d) Trends in Enthalpy of Formation of Spinels

The enthalpies of formation of 2–3 cubic oxide spinels from component oxides are presented in Fig. 5 as a function of the atomic number of the divalent cation. The data for different families of spinels based on the common trivalent cation follow ap-

proximately parallel curves. For aluminate and chromite spinels, information from both calorimetric measurements (*18, 19*) and emf are shown. The general agreement between the two adds credence to the second-law entropies derived from emf studies.

The curve for vanadites normalized on known data on FeV_2O_4 and CoV_2O_4, suggests that the heat of formation of CuV_2O_4 is 23 (±3) kJ mole^{-1}. With such a high positive enthalpy of formation, it is unlikely that this compound would be stable. Further, as seen from Fig. 3, the oxygen potentials corresponding to the existence of Cu^{2+} ions are much higher than those corresponding to the existence of V^{3+} ions. On both thermodynamic and valence considerations, it appears unlikely that CuV_2O_4 can be synthesised as a pure compound.

Since the enthalpy of formation of NiV_2O_4 is slightly negative (Fig. 5), and the compound is expected to be entropy stabilized on the basis of site preference energies of Ni^{2+} and V^{3+} ions, the free energy of formation of NiV_2O_4 from NiO and V_2O_3 is expected to be negative for all temperatures. Valency considerations (Fig. 3) also do not preclude the formation of NiV_2O_4. Earlier unsuccessful attempts (*20, 21*) to prepare NiV_2O_4 can be understood in the light of the phase diagram proposed by Gianoglio and Ramonda (*22*) for the Ni–V–O system at 1073 K, which shows significant solid solubility of Ni in V_2O_3. The phase mixture $(V,Ni)_2O_3$ + NiO + Ni appears to be more stable than NiV_2O_4.

Acknowledgments

The authors wish to thank Mr. N. Venugopal Rao and Mr. A. V. Narayan for assistance in the preparation of this manuscript.

References

1. W. Kunnmann, D. B. Rogers, and A. Wold, *J. Phys. Chem. Solids* **24,** 1535 (1963).
2. K. T. Jacob and C. B. Alcock, *Met. Trans. B* **6,** 215 (1975).
3. K. T. Jacob, *J. Mater. Sci.* **15,** 2167 (1980).
4. K. Kiukkola and C. Wagner, *J. Electrochem. Soc.* **104,** 379 (1957).
5. E. Aukrust and A. Muan, *Trans. AIME* **227,** 1378 (1963).
6. V. J. D. Tretjakow and H. Schmalzried, *Ber. Bunsenges. Phys. Chem.* **69,** 396 (1965).
7. J. Myers and W. D. Gunter, *Amer. Mineral.* **64,** 224 (1979).
8. M. W. Chase et al., Supplement to JANAF Thermochemical Tables, *J. Phys. Chem. Ref. Data* **3,** 412 (1974).
9. M. Wakihara and T. Katsura, *Met. Trans.* **1,** 363 (1970).
10. T. Katsura and M. Hasegawa, *Bull. Chem. Soc. Japan* **40,** 561 (1967).
11. J. C. Chan, C. B. Alcock, and K. T. Jacob, *Canad. Met. Quart.* **12,** 439 (1973).
12. K. T. Jacob, *Thermochim. Acta* **15,** 79 (1976).
13. K. T. Jacob and J. Valderrama-N, *J. Solid State Chem.* **22,** 291 (1977).
14. K. T. Jacob, *J. Electrochem. Soc.* **124,** 1827 (1977).
15. J. D. Dunitz and L. E. Orgel, *J. Phys. Chem. Solids* **3,** 318 (1957).
16. K. T. Jacob, unpublished research.
17. D. R. Stull et al., "JANAF Thermochemical Tables," NSRDS-NBS 37 (1971).
18. A. Navrotsky and O. J. Kleppa, *J. Inorg. Nucl. Chem.* **20,** 479 (1968).
19. F. Muller and O. J. Kleppa, *J. Inorg. Nucl. Chem.* **35,** 2673 (1973).
20. G. Blasse and E. W. Gorter, *J. Phys. Soc. Japan* **17,** Suppl. B.I., 176 (1962).
21. D. B. Rogers, R. J. Arnott, A. Wold, and J. B. Goodenough, *J. Phys. Chem. Solids* **24,** 347 (1963).
22. C. Gianoglio and G. Ramonda, *Rev. Int. Hautes Temp. Refract.* **10,** 27 (1973).